Large area mapping of annual land cover dynamics using multi-temporal change detection and classification of Landsat time series data

Steven E. Franklin[1], Oumer S. Ahmed[2]*, Michael A. Wulder[3], Joanne C. White[3], Txomin Hermosilla[4], and Nicholas C. Coops[4]

Affiliations:

[1] Department of Environmental and Resource Studies/Science, Department of Geography, Trent University, Ontario, K9J 7B8, Canada

[2] Geomatics, Remote Sensing and Land Resources Laboratory, Department of Geography, Trent University, Ontario, K9J 7B8, Canada

[3] Canadian Forest Service (Pacific Forestry Centre), Natural Resources Canada, 506 West Burnside Road, Victoria, British Columbia, V8Z 1M5, Canada

[4] Integrated Remote Sensing Studio, Department of Forest Resources Management, University of British Columbia, 2424 Main Mall, Vancouver, BC V6T 1Z4, Canada

* Corresponding author:

E-Mail address: osahmed@trentu.ca;

Tel.: 705-748-1011 x 6111.

Pre-print of published version.

Reference:

Franklin, S.E., Ahmed, O.S., Wulder, M.A., White, J.C., Hermosilla, T., Coops, N.C. (2015). Large area mapping of annual land cover dynamics using multi-temporal change detection and classification of Landsat time series data.

DOI: http://dx.doi.org/ 10.1080/07038992.2015.1089401

Abstract

Land cover characteristics remain of particular interest to the monitoring and reporting communities, and approaches for generating annual maps of land cover informed by change information derived from long time series are critically needed. In this study, we demonstrate and verify the utility of disturbance and recovery metrics derived from annual Landsat time series to inform the classification of annual land cover over a >1.2 million hectare forest management area in the Boreal Mixedwood Region of northern Ontario, Canada. Annual land cover maps were generated, producing temporally-informed products and compared to the established approach of using single-date spectral variables and indices. The Random Forest (RF) classification algorithm was used to classify land cover annually between 1990 and 2010, followed by the application of an annual temporal filter to remove illogical land cover transitions. Change detection in the study area had an overall accuracy of 92.47%. The use of time series metrics in the classification of land cover improved overall accuracy by 6.38% compared to single-date results. Using a separate independent reference sample, the RF classification approach combined with post-classification transition filtering, resulted in an overall classification accuracy of 87.98%. The use of annual change and trend information to guide land cover, which is further informed by logical land cover transition rules, points to the creation of efficient, robust, and reliable land cover products in a transparent and operational fashion.

1.0 Introduction

The interpretation of annual land cover dynamics based on the analysis of remote sensing change detection and land cover classification maps across large areas and long time periods is an important natural resource management requirement (Lambin et al., 2003; Wulder and Franklin 2007, Roy et al., 2014). These activities are now feasible and facilitated by the free and open access to the entirety of the United States Geological Survey Landsat archive (Woodcock et al., 2008) in a readily accessible form (Wulder et al. 2012). Access to this tremendously rich archive creates new opportunities to detect vegetation changes at higher temporal frequency and at more detailed spatial scales than was previously possible in many areas (e.g., Huang et al., 2010; Kennedy et al., 2010; Zhu and Woodcock 2014), with Canada especially well represented with imagery (White and Wulder 2013). In actively managed forested areas, the annual assessment of Landsat time series data can be used to interpret detailed disturbance history and land cover changes (Sexton et al., 2013). Such an interpretation is also particularly useful in carbon modelling (e.g., Turner et al., 2004; Goward et al., 2008), and in characterizing forest change in a manner that is more consistent with detection of natural and human influences on ecological condition and processes (e.g., Kennedy et al., 2014). Carbon balance, whether based on models or inventory, is highly dependent on the land cover since it affects several directly relevant characteristics such as albedo, emissivity, photosynthetic potential, and transpiration (Zhu and Woodcock 2014). Unique information produced from time series detection of change includes spectral clues on succession (Pflugmacher et al. 2012) and post-disturbance recovery (Hermosilla et al. 2015). Additionally, annual land cover derived from Landsat can be used to produce a series of carbon model relevant variables such as pre-disturbance and post-disturbance land cover which are also of general interest to monitoring, inventory, and reporting programs. This type of information is important to inform carbon models but conventionally difficult to derive when applying standard two-date change detection and single date land cover classification methods.

Annual land cover classification maps produced from dense Landsat time series data in specific areas enhance the interpretation of forest and land cover dynamics when used together with more

spatially comprehensive, but often less frequently produced, Landsat-based single-image date land cover products and compilations of multiple imagery (such as those used to create national or regional vegetation inventory data). For example, in Canada, among the most widely used national land cover maps is the Earth Observation for Sustainable Development of Forests product (typically referred to as EOSD LC 2000). This Landsat-based map provides a national land cover database of the forested area of Canada with 23 land cover classes for the year circa 2000. Annual land cover classification products are an ideal addition to the established EOSD LC 2000 maps which have, in Canada and in similar large area coverages in other jurisdictions, been used to inform reporting programs (Wulder et al. 2004; Kangas and Maltamo 2006) and allow for the implementation of unique science activities (e.g., Wulder et al. 2011; Yemshanov et al. 2011).

Annual land cover classification using Landsat time series data has fostered the use of specific disturbance- or recovery-based metrics in the classification procedure (Hansen and Loveland 2012). Vegetation dynamics and forest cover changes identified using the 'greatest change metric', or similar disturbance- or recovery-based metrics, attempt to identify vegetation dynamics that occur prior to the date of the image classification (e.g., Roy et al., 2014). The composition of land cover at any point in time is linked to its disturbance history. Therefore, inclusion of the disturbance-related variables is expected to increase the land cover classification accuracy over that which can be obtained using single-date spectral variables. In addition, by using the change metrics to inform the classification, it is possible to provide a single land cover class for a given pixel for the entire period when change is not specifically identified and there is no spectral evidence to indicate otherwise.

The use of these disturbance- or recovery-based metrics also implies an increment in the dimensionality of the data sets being used in image classification. This increase in dimensionality can compromise the capability of traditional multispectral classifiers, but can be addressed by the selection of a robust classifier or an ensemble of machine-learning algorithms, such as the Random Forest (RF) package (Dietterich 2000). The RF approach, in particular, has received notable attention because it has flexibility with regards to the nature and distribution of input variables and has been found to be

robust in situations problematic to traditional classifiers (Liaw and Wiener 2002). Recently, this been buttressed in the use of disturbance- and recovery-based metrics extracted by time series trajectory-based methods to characterize forest change and estimate (via modelling) forest biophysical properties (Ahmed et al., 2015; Pflugmacher et al., 2012). The basic approach is based upon detection of change in surface reflectance and classification of such changes in terms of land cover change or by characterizing trends (for more subtle discontinuous phenomena, such as partial land cover change or re-growth, see Meigs et al. (2011)).

In this study, we present an approach for integrated change detection and land cover mapping with the aim of informing forest inventory and carbon accounting programs. Our method is novel in that it integrates: 1) annual large-area composites that contain no spatial or temporal data gaps; 2) predictor variables that correspond with disturbance and recovery conditions; 3) output as medium resolution annual land cover maps; and 4) a Random Forest classifier that is robust in case of heterogeneous classes and reference data error. Finally, we provide an indication of future improvements in the methods based on an analysis of both i) land cover change over time, and ii) other changes that are captured in the Landsat time series in related disturbance- or recovery-based metrics. This latter improvement will facilitate an interpretation of more subtle changes within a specific land cover, such as a pattern of smaller though still significant changes, or through analysis of repeated land cover transitions (e.g., cyclical change).

2.0 Data and Methods

In this study, we created and interpreted annual Landsat time-series land cover classification and change detection maps that cover the period 1990-2010 in the Hearst Forest in northern Ontario, Canada. We incorporated various forest disturbance- and recovery-based metrics available from the image time series into the land cover classification process, and create land cover change detection maps based on an analysis of the ‘greatest change’ in the time series. We then developed a land cover transition matrix to relate the observed ‘greatest change’ locations to specific land cover changes, such as a change in conifer or mixedwood forest land cover subsequent to clearcut harvesting activities. To

assess accuracy of the change detection, we compared the results of these land cover change outcomes to an independent reference dataset created via interpretation of the Landsat time series imagery. We evaluated the accuracy of the land cover classification using visual interpretation of both the Landsat time series and aerial photography. The sampling design for selection of reference samples was a probability-based design such that the probability of selecting each land cover class is known and it is sensitive to rare classes (Olofsson et al., 2014). The flowchart in Figure 1 summarizes the overall approach of this study described in the following sub-sections.

2.1 Study area

The study area is the Hearst Forest Management Area located in northern Ontario (see Figure 2). This area is an actively managed, commercial forest that is found within the Boreal Mixedwood ecozone, and covers approximately 1.23 million ha (of which, approximately 1 million ha are productive forest (Hearst Forest Management Inc. 2011)). The Hearst Forest is dominated by coniferous tree species, with black spruce *(Picea mariana* Mill. B.S.P.) representing 67% of gross volume in the area. Jack pine (*Pinus banksiana* Lamb.), white spruce (*Picea glauca* Moench Voss), balsam fir (*Abies balsamea* L. Mill.) and tamarack (*Larix laricina* Du Roi K. Koch) are also represented. Deciduous species in this region include white birch (*Betula papyrifera* Marsh.), trembling aspen (*Populus tremuloides* Michx.) and balsam poplar (*Populus balsamifera* L.). Approximately 60,000–70,000 ha of forest is harvested annually from this area using a variety of methods, including clearcutting (Hearst Forest Management Inc. 2007). With an active fire suppression program successfully controlling or limiting the effects of wildfire, timber harvesting is the most common form of disturbance in the Hearst Forest; however, large fires were recorded in 1995 and 1996. Insect outbreaks have also occurred in the area; for example, a spruce budworm outbreak occurred in 1999. Recent harvesting, fire history, and other disturbance events (e.g., insect outbreaks) in the area are described in the Hearst Forest Management Plan (2007-2017) published by Hearst Forest Management Inc. (2011).

2.2 Best-available pixel (BAP) image composites and change metrics

The Landsat imagery for the study area was obtained from the United States Geological Survey (USGS) Landsat archive. The study area intersects six Landsat WRS-2 path / rows. A total of 706 Landsat images acquired between 1988-2012, to represent 1990-2010 conditions, were used to create multi-temporal pixel-based image composites using a best-available-pixel (BAP) approach (implementing the methods described by White et al. (2014)), and is briefly summarized here: First, atmospheric correction was applied to all images using the Landsat Ecosystem Disturbance Adaptive Processing System (LEDAPS) algorithm (Masek et al., 2006; Schmidt et al., 2013) transforming digital numbers into surface reflectance values. Second, clouds, cloud shadows and water were detected and masked using the Function of mask (Fmask) algorithm (Zhu & Woodcock, 2012). Once pre-processing was complete, candidate pixel observations were scored according to sensor, acquisition day of year (DOY), distance to clouds and cloud shadows, and atmospheric opacity. A target day of year DOY of August 1 (Julian day 213) was selected within the growing season, and the date range for candidate images was restricted to ± 30 days. In the final step, the pixels with the highest score were used to populate the final image composite, and the surface reflectance values for these best observations were then written in the annual BAP composite. This method allows the production of spatially contiguous, cloud-and haze-free, spatially consistent temporal series of surface reflectance composites of Landsat data. Based upon the rules applied, instances of no valid pixels for inclusion in the composite occurred. For example, pixel locations in the annual BAP composites with observations from images acquired outside ±30 days of the target DOY were assigned a “no data” value. Similarly, noisy or anomalous pixel values (spikes in the temporal pixel series) were also identified and assigned a “no data” value as described in Hermosilla et al. (2015). In our study, infilling of data gaps (pixels with “no data” values) was performed using the proxy value composite approach (Hermosilla et al., 2015). Briefly, this approach detects spectral change and derives a series of metrics characterizing these spectral changes, and then uses these change metrics to aid in proxy value assignment. Here the “greatest change” metric was used to flag disturbance events. Then, data

gaps were filled by considering the full spectral information of the pixel time series; proxy values are informed by those from preceding and/or following dates, and these no-data pixels are replaced with values that are most spectrally similar in time and space. Replacement of these values is desired to enable production of gap-free spatially exhaustive annual proxy value composites that are spectrally consistent in order to support the production of annual land cover products. Our annual land cover classification was based on these proxy BAP composites and a series of disturbance- and recovery-based change metrics that are derived using a breakpoint detection process performed informed by the Normalized Burn Ratio (NBR) on a temporal pixel series (as per Hermosilla et al., 2015). The breakpoint detection process, in this study, is performed over the Normalized Burn Ratio (NBR) pixel series, which has been demonstrated as sensitive and consistent for the retrieval of disturbance events over forest environments (Kennedy et al., 2010). The trends that can be computed after implementation of the breakpoint detection process are of distinct types. In this study, we used the 'greatest negative change' in the time series, to derive a set of descriptive change metrics. This "greatest change" metric allowed us to characterize the change events as well as conditions pre- and post-the change. The metrics relay information on change year, magnitude, and duration are grouped into pre-change, at the time of change, and post-change categories. These change metrics characterize the negative breakpoint segments using: year, magnitude, and duration. Table 1 provides a complete listing, categorized by type, of all the spectral inputs derived from the BAP composites that were used as inputs for the land cover classification. Elevation information, derived from a DEM, was the only non-composite input data used for the classification.

2.3 Ancillary data

There are several approaches for incorporating ancillary data in the image classification process based on earlier studies that incorporated DEM data into land cover classification (e.g., Janssen et al., 1990) to approximate differing ecosite conditions. In this study, several tiles of the Canadian Digital Elevation Data (CDED) DEM were downloaded from the GeoBase online spatial data portal (www.geobase.ca) to be used in the land cover classification.

High spatial resolution colour-infrared leaf on aerial orthophotography was acquired in 2007 at approximately 1:20000 scale with 40cm resolution covering most of the Hearst forest. This aerial orthophotography was used to collect calibration and reference data for each land cover class. An existing land cover product was used to provide strata for selection of calibration and reference samples. The Earth Observation for Sustainable Development of Forests product (EOSD LC 2000) is a land cover product representing the forested area of Canada circa 2000, with 23 land cover classes. Details on the land cover map can be found in Wulder et al. (2008). A stratified random sample was used with the EOSD LC 2000 map providing an initial stratification to estimate the proportions of each land cover class over the entire area of the Hearst Forest to guide the proportion of training and reference samples (Wulder et al., 2006). Eight classes in the EOSD LC 2000 land cover map product were selected to characterize land cover in the Hearst Forest (mixedwood forest, coniferous forest, herb, wetland treed, broadleaf forest, wetland, water and exposed land). These classes dominate the area as per the EOSD land cover classification map product (note that these classes are derived from EOSD LC 2000 Level 4, which does not include forest density classes). Sampling strata were generated from the EOSD LC 2000 map, which enabled estimation of proportions of each land cover class over the entire area of the Hearst Forest to guide the sample composition and selection.

2.4 Change detection validation

The accuracy assessment of the change detection approach relied on independent reference data collected through visual interpretation of the Landsat time series imagery and the 2007 1:20000 scale colour-infrared aerial photography (see Stehman and Czaplewski, 1998, Cohen et al., 2010; Cohen et al., 1998; Kennedy et al., 2007; Masek et al., 2008; Huang et al., 2009). A stratified random sample design was used to select 100 samples (pixels) from the change and no change strata for a total of 200 reference pixels used to evaluate the accuracy of change detection. For each sample, the BAP composites were visually examined for the years immediately preceding and following the greatest change year. In addition, the 2007 aerial photography was also examined, and the accuracy assessment results were recorded.

2.5 Land cover calibration and validation

A stratified random sampling approach was used to acquire land cover classification calibration and reference data for each of the land cover stratum generated from the EOSD LC 2000 data. Sample size determination for reference purposes invariably involves tradeoffs between the requirements of statistical rigour and logistical realities (Czaplewski & Patterson, 2003; Wulder, et. al., 2007). The number of samples required for reference was determined using a 95% confidence interval for p with a margin of error of 5%, and an assumption of 80% true accuracy (Cochran, 1977; Wulder, et al., 2007), resulting in a sample size of 174. Half of these samples were allocated proportional to the area of the classes (from EOSD LC 2000), whilst the other half was used to improve estimates for rare classes. For each sample, the land cover class in 2007 was interpreted from the aerial photography according to the same classification hierarchy as the EOSD product (Wulder et al., 2008). An additional 406 photo-interpreted samples were selected for model calibration and were allocated in the same manner (half proportional to area of each EOSD class; half for rare classes) (Table 2). All of the calibration and reference samples were selected in areas where land cover was unchanged throughout the time period of the analysis (1990–2010).

In this study, for accuracy assessment of change detection and land cover outputs the approach which adjusts class area estimates for misclassification error was adopted as described by Card (1982) since it fits with recommended good practice for the accuracy assessment and use of land cover maps derived from remote sensing (Olofsson et al., 2013, 2014). In this approach the misclassification error adjusted estimates of area are derived from the confusion matrix which forms the basis for the estimation of map accuracy.

2.6 Classification algorithm

The Random Forest (RF) algorithm was selected because of its relatively high accuracy and computational efficiency (Brieman 2001). The dependent variable – one of the eight classes – was predicted using the independent variables of Landsat spectral variables and indices, DEM and time-

series metrics. The RF classifier consists of an ensemble of tree-based classifiers, it uses bootstrap samples with replacement to grow a large collection of classification trees, which assign each pixel to a class based on the maximum number of votes that a class receives from the collection of trees. Each tree is grown from a randomly and independently selected subspace (i.e., a certain proportion of pixels) of the measurement space (training pixels) that is used to train the RF classifier; the remaining samples (called out-of-bag cases) are used to assess the accuracy of the classification. Two parameters must be specified: (i) the number of trees to grow, and (ii) the number of randomly selected split variables at each node (mtry). The default number of trees (500) was used since values larger than the default are known to have little influence on the overall classification accuracy (Breiman and Cutler, 2007). The other adjustable RF tuning parameter, the mtry parameter, controls the number of variables randomly considered at each split in the tree building process, and is believed to have a "somewhat sensitive" influence on the performance of the RF algorithm (Breiman and Cutler, 2007). For categorical classifications based on the RF algorithm, the default value for the mtry parameter is $\sqrt{p}$, where p equals the number of predictor variables within a data set (Liaw and Wiener, 2002). Model building and tuning were performed using version 3.0.3 of the 64-bit version of R (R Development Core Team, 2014). Several add-on packages were used within R to create the final classification, which relied on the "RandomForest" package (Liaw and Wiener, 2002, Breiman and Cutler, 2007, Breiman, 2001).

2.7 Reference year land cover classification

RF and the aforementioned calibration samples were used to produce a land cover classification for 2007. The 2007 reference date was selected based on the availability of near-coincident land cover validation data in the form of colour-infrared aerial orthophotography at 1:20000 scale. Two different classification scenarios were explored (Table 1). In the first classification scenario, we used single-date spectral variables and derived spectral indices as inputs to RF. In the second classification scenario, we used the same set of single date inputs as were used in scenario 1, with the addition of change metrics derived from trajectory analysis of our stack of annual BAP proxy image composites (Tables 2 and 3).

2.8 Temporal transition filtering

The RF model with the greatest overall classification accuracy, as evaluated following the approach outlined in Section 2.5, was applied to each year of the BAP proxy composite imagery. Post-classification, the annual land cover classifications were evaluated to identify and remediate illogical land cover transitions using a temporal filter (e.g., Sexton et al. 2013). We defined illogical land cover transitions as those transitions that make no ecological sense in the context of the study area. An example of an illogical transition would be from coniferous land cover to exposed land cover to coniferous land cover in the span of only three years. The temporal filter was a 3-year moving window applied to each pixel through the time series, beginning in 1990 and proceeding annually to 2010. The filter was advanced year by year in the temporal sequence, and when an illogical transition was encountered, the land cover class from the previous year was automatically used to replace the current year's land cover. We then evaluated the impact that this post-classification temporal transition filtering had on the accuracy of the reference year land cover classification.

3.0 Results and Discussion

3.1 Change detection validation

The accuracy of land cover change detection is reported in Table 3. Overall accuracy was 92.47% with a margin of error of ± 3.66%. Commission and omission errors for change events were 12.00% and 7.37% respectively. Figure 3 shows all of the change events detected in the Hearst Forest for the period 1990–2010. Of the approximately 24 million pixels in the Hearst Forest, approximately 2 million (or 10%) experienced a land cover change event during the two decades represented in the Landsat time series. The accuracy result indicates more omission errors than commission errors in detected changes. There is no noticeable trend in the spatial pattern of errors. The omission errors could result from partially changed pixels. Such pixels are usually difficult to detect, as the magnitude of change is mostly reliant on the proportion of change within that pixel.

3.2 Land cover validation

Two different land cover classification scenarios were explored for the 2007 reference year, using two different sets of input variables for modelling (Table 1). The 2007 classifications were validated using high resolution colour aerial photography acquired in 2007 (Section 2.3) and 174 reference samples (Section 2.5). The accuracy assessment results for the first 2007 classification scenario, which used single-date inputs, are summarized in Table 4, whilst the results for the second scenario, which incorporated single date inputs and time series change metrics are summarized in Table 5. Incorporation of the change metrics improved overall classification accuracy for 2007 from 79.38% to 85.77% and reduced the margin of error by 0.82%. Omission errors for scenario 2 were lower for all classes except water, and wetland, which were the same for both scenarios. The greatest decrease in omission error in scenario 2 relative to scenario 1 were for the broadleaf and exposed land classes. Similarly, commission errors were lower for scenario 2, particularly for the exposed land, wetland treed, and mixedwood classes. The mixedwood forest class, which represents approximately 41% of the Hearst Forest area, had an estimated user's accuracy of 84.75% for scenario 2, compared to 71.88% for scenario-1.

Based on these results, the scenario 2 classification model was selected for application to all other years in the time series (1990–2010). Figure 4 shows the 2007 reference land cover classification map (scenario 2) for the Hearst Forest with the eight land cover classes. An estimate of variable importance (VI), as provided by the Random Forest algorithm, is shown in Figure 5. VI is estimated by randomly permuting the variable in the out-of-bag (OOB) samples; an increased out-of-bag error is an indication of the importance of that variable to the model, providing indication how influential an input variable is on the overall accuracy (Genuer et al., 2010). VI is measured with mean decrease in accuracy (MDA), to calculate the MDA of a variable, the values of the variable are randomly permuted for the OOB data, while keeping the values of the other variables constant. The importance of the variable is obtained by comparing the resulting misclassification rate with the rate achieved without randomly permuting the values of the variable. This procedure is repeated for each variable (Breiman, 2001).

The top five most important variables were single date Landsat spectral variables and spectral indices, with the next most important three variables selected from among the Landsat-based time-series change metrics (trend magnitude, greatest disturbance duration, and post-disturbance duration).

3.3 Final classification and land cover transitions

The annual land cover classifications were produced by applying the RF model developed in scenario 2 for the reference year to all other years in the time series. Then, we examined all of the annual land cover classifications and assessed land cover transitions. Temporal transition filtering was performed to remove illogical class transitions, and the transitions that were considered illogical in the context of the study area are summarized in Table 6. The application of the filtering process allowed us to estimate the gain in classification accuracy from our post-classification transition-rule filtering. The accuracy assessment results for the 2007 filtered classification are summarized in Table 7. When compared to the results for the scenario 2 reference classification for 2007 (Table 5), the overall accuracy was improved 2.2% as a result of the temporal transition filtering, whilst the margin of error was reduced by 0.36%. With the exception of the wetland treed and mixedwood classes, omission errors were the same or lower for the transition filtered classification, particularly for the wetland class. Commission errors were likewise reduced or the same for the filtered classification for most classes, but increased for wetland treed.

The time series of filtered annual land cover classifications were then used to characterize general land cover transformations in the Hearst Forest over the past 20 years. Figure 6, 7 and 8 illustrate examples of land cover transitions identified in the study; shown are the colour-infrared aerial photography, normalized burn ratio (NBR), land cover changes over the 1990-2010 time period, eight class land cover classification for 2007, and a summary change transition map. Also shown in Figure 6 are four smaller sample sites (numbered 1-4), which are used in Figure 7 and 8 to illustrate different land cover change transitions in the study area.

Sites 2 and 4 were disturbed early in the time series 1991 and 1997, respectively; sites 1 and 3 are more recent disturbances (2006 and 2005, respectively). These sites were selected to show typical land

cover transition characteristics that are found in the study area. It can be seen from the summary land cover transition map (Figure 6) that many of the pixels that were disturbed early in the time series had recovered by the end of the time series. Of the approximately 10% of the study area that was identified as experiencing land cover change, more than 90% had recovered by 2010. The remaining areas show as herb or exposed land class in 2010 (See Figure 7). Examples of land cover transitions in areas shown in Figure 7a and 7b show site 2 from Figure 6 in greater detail. Site 2 contains an area that was harvested at the beginning of the available time series; the dominant land cover class at the start of the time series was coniferous, as a result of harvesting, the majority of the area was converted to exposed land and then transitioned to herb, and eventually the site recovered to mixedwood. The graph in 7b shows a pixel located near the edge of this harvest block (labelled as # 1 in 7a) that transitioned from coniferous to exposed land then to herb and finally to mixedwood. Figure 8a and 8b show site 3, which displays also a complex series of land cover transitions: the area was harvested in 2004 and 2005, and most of this area transitioned from exposed land (post-harvest) to different land cover classes by the end of the time series in 2010. The graph (Figure 8b) shows an example of a pixel that was labelled as conifer at the beginning of the time series, was later classified as exposed land, and then experienced a transition over the next few years from herb to mixed wood.

Table 8 summarizes the land cover transitions in the Hearst forest, by 5-year epochs, from 1990 to 2010. These five year epochs were selected to illustrate broad land cover change patterns within the 20 year time interval examined for this study. Note that only pixels that changed land cover at some point – not necessarily from the beginning to the end of the time period, but at least once during the epoch - were tabulated in each epoch. Most land cover change pixels experienced only one land cover change in the 20 year time period. However, some pixels started a given epoch in one land cover class, changed to a different class, and then returned to the original class by the end of that five year epoch. The percentage of these pixels are counted in Table 8 as having changed from one class and returning to that class.

Approximately 10% of the study area (about 6000 hectare) are represented in these tables (i.e. areas that have experienced land cover change); of these, many of the land cover transitions were made to the herb land cover class from one of the forest classes. This occurred in each five year epoch. For example, of the 408 hectare mixedwood identified as having changed in the first epoch (in Table 8a), approximately 28.61% remained as mixedwood at the end of the epoch (despite having undergone a change in land cover class typically during the earlier part of the epoch). Another approximately 51.6% of this area originally classified as mixedwood changed to herb in the first epoch. Similarly, of the areas that began the first five year epoch as conifer, and experienced a land cover transition during this epoch, approximately 23.9% returned to conifer by the end of the time epoch in 1995. In the same epoch, approximately 10.19% and 56.53% of these conifer land cover change pixels changed land cover to the mixedwood and herb classes, respectively. The exposed land cover pixels also show a reasonable land cover change trend over the first epoch; of the 25.8 hectare that began the first five year epoch classified as exposed land, approximately 34.23% experienced a land cover change (typically to the herb class) but remained or returned to the exposed land class by the end of the 5 year epoch. Approximately 16.2% and 35.99% of the exposed land pixels were classified as mixedwood and herb by the end of the first epoch.

There are clear patterns of change between mixedwood, coniferous and herb land cover classes in each epoch and over the 20 year time period. The transitions between these classes appear to represent land cover change and dynamics associated with harvesting activities (e.g., clearcutting conifer to exposed to herb) and forest regeneration (e.g., herb to mixedwood). The annual land cover classification helps to confirm interpretations of the kind of land cover change occurring on an annual basis and over time for the entire study area. A compilation of the annual percentage of different land cover classes throughout the time series is contained in Figure 9. This classification method can be applied to other areas to produce spatially and temporally consistent information on annual land cover, providing sufficient archived Landsat data is available. The approach allows the use of spatially contiguous, cloud-and haze-free, spatially consistent temporal series of Landsat data for large area land

cover mapping. The resulting information on land cover dynamics is important for the study of carbon modeling. Spatially explicit carbon modeling methods often require information on annual land cover and land cover changes, especially such that can be portrayed in a change matrix. The pre-disturbance land cover, the year of disturbance, and the post-disturbance land cover class information, can be joined with data on carbon dynamics to estimate carbon stocks, stock changes, and the associated emissions and removals over time. Future research is intended towards the implementation of land cover classification approaches using all available Landsat imagery to assess intra-annual phenological change and to test this approach for other regions with different environments. Further, knowing the variable yield of imagery that can be expected within a given year or growing season, opportunities such as implemented by Senf et al. (2015) using multi-scale applications also merit additional investigation.

4.0 Conclusions

In this study, annual land cover maps were generated from a time series of Landsat image composites for the period 1990-2010 in the Hearst Forest in northern Ontario. Time series trajectory analysis identified areas that had changed land cover at least once during the 1990–2010 time period based on the ‘greatest change metric’; such areas were then filtered for illogical transitions, examined for land cover change patterns, and interpreted in context of known forest management practices and land cover transitions. Incorporation of change metrics derived from the time series into the land cover classification approach improved overall accuracy by 6.38% compared to single image date results. Subsequent post-classification filtering of the time series of annual land cover classifications further improved overall accuracy by an additional 2.2%. The capacity to characterize land cover transitions through time is a unique contribution of this study. For example, mixedwood forest that experienced change early in the time series showed a typical vegetation transition pattern: mixedwood transitioned to exposed land following harvest, then transitioned to herb, and subsequently returned to mixedwood by the end of the time series. An area that was more recently disturbed changed from conifer to exposed land and then to herb. Such characterizations of land cover transitions rely on both the

accurate detection of change events, as well as the accurate classification of land cover. Future work will examine conversion of these transitions into inputs relevant for carbon budget modelling, such as pre-disturbance and post-disturbance land cover. These interpretations of land cover dynamics are also of general interest to monitoring, inventory, and reporting programs, as well as characterizing post-disturbance recovery trajectories.

5.0 Acknowledgements

This research was supported by the Natural Science and Engineering Research Council of Canada and via the “National Terrestrial Ecosystem Monitoring System (NTEMS)" project jointly funded by the Canadian Space Agency (CSA) Government Related Initiatives Program (GRIP) and the Canadian Forest Service (CFS) of Natural Resources Canada.

6.0 References

Ahmed, O.S., Franklin, S.E., Wulder, M.A., White, J.C. 2015. Characterizing Stand-Level Forest Canopy Cover and Height Using Landsat Time Series, Samples of Airborne LiDAR, and the Random Forest Algorithm. ISPRS Journal of Photogrammetry and Remote Sensing, Vol. 101, pp. 89-101. DOI: http://dx.doi.org/10.1016/j.isprsjprs.2014.11.007.

Bivand, R. S., Pebesma, E. J., Gomez-Rubio, V. 2013. Applied spatial data analysis with R, Second edition. Springer, NY. http://www.asdar-book.org/

Breiman, L. 2001. Random Forests. Machine Learning, 45, 5–32.

Breiman, L., and Cutler, A. 2007. Random forests — Classification description. : Random forests Available at: http://stat-www.berkeley.edu/users/breiman/RandomForests/cc_home.htm [Accessed November 27, 2014].

Card, D.H., 1982. Using known map category marginal frequencies to improve estimates of thematic map accuracy. Photogrammetric Engineering and Remote Sensing, Vol. 49, pp. 431–439.

Cochran, W. G. 1977. Sampling techniques, 3rd Edition New York: John Wiley & Sons 428.

Czaplewski, R. L., and Patterson, P. L. 2003. Classification accuracy for stratification with remotely sensed data. Forest Science, Vol. 49, pp. 402 − 408.

Dietterich, T.G. 2000. An Experimental Comparison of Three Methods for Constructing Ensembles of Decision Trees: Bagging, Boosting, and Randomization. Machine Learning, Vol. 40, pp. 139-157.

Genuer, R., Poggi, J. M., Tuleau-Malot, C. 2010. Variable selection using random forests. Pattern Recognition Letters, Vol. 31, pp. 2225–2236.

Goward, S. N., Masek, J. G., Cohen, W., Moisen, G., Collatz, G. J., Healey, S., et al., 2008. Forest disturbance and North American carbon flux. Eos, Vol. 89, 11.

Hansen, M. C. and Loveland, T. R. 2012. A review of large area monitoring of land cover change using Landsat data. Remote Sensing of Environment, Vol. 122, pp. 66-74.

Hearst Forest Management Inc. 2011. Current Forest Condition. Available online: http://www.hearstforest.com/english/current.html (accessed on 20 April 2014).

Hearst Forest Management Inc. 2007. Forest Management Plan for the Hearst Forest; Hearst Forest Management Inc.: Hearst, ON, Canada.

Hermosilla, T., Wulder, M. A., White, J. C., Coops, N.C., Hobart, G. 2015. An integrated Landsat time series protocol for change detection and generation of annual gap-free surface reflectance composites. Remote Sensing of Environment, Vol. 158, pp. 220-234.

Huang, C., Goward, S. N., Masek, J. G., Thomas, N., Zhu, Z., and Vogelmann, J. E. 2010. Anautomated approach for reconstructing recent forest disturbance history using dense Landsat time series stacks. Remote Sensing of Environment, Vol. 114, pp. 183–198.

Janssen, L.F., Jaarsma, J. and van der Linder, E. 1990. Integrating Topographic Data with Remote Sensing for Land-Cover Classification, Photogrammetric Engineering & Remote Sensing, Vol. 56, pp. 1503-1506.

Kangas, A. and Maltamo, M. (Eds.) 2006. Managing Forest Ecosystems: Forest Inventory: Methodology and Applications. Dordrecht, Netherlands: Springer.

Kennedy, R. E., Cohen, W. B., and Schroeder, T. A. 2007. Trajectory-based change detection for automated characterization of forest disturbance dynamics. Remote Sensing of Environment, Vol. 110, pp. 370–386.

Kennedy, R. E., Andréfouët, S., Cohen, W. B., Gómez, C. et al., 2014. Bringing an ecological view of change to Landsat-based remote sensing. Frontiers in Ecology and Environment doi:10.1890/130066

Kennedy, R. E., Yang, Z., and Cohen, W. B. 2010. Detecting trends in forest disturbance and recovery using yearly Landsat time series: 1. LandTrendr—Temporal segmentation algorithms. Remote Sensing of Environment, Vol. 114, pp. 2897–2910.

Lambin, E., et al., 2003. Dynamics of Land Use and Land Cover Change in Tropical Regions. Ann. Review.Env. Resour., 28:205-241.

Liaw, A., & Wiener, M. 2002. Classification and regression by randomForest. R News, 2(3), 18–22.

Masek, J. G., Vermote, E. F., Saleous, N. E., Wolfe, R., Hall, F. G., Huemmrich, K. F., et al., 2006. A Landsat surface reflectance dataset for North America, 1990–2000. IEEE Geoscience and Remote Sensing Letters, 3(1), 68–72.

Meigs, G. W., Kennedy, R. E., Cohen, W. B. 2011. A Landsat time series approach to characterize bark beetle and defoliator impacts on tree mortality and surface fuels in conifer forests. Remote Sensing of Environment, Vol. 115, pp. 3707–3718.

Olofsson, P., Foody, G.M., Stehman, S.V., Woodcock, C.E., 2013. Making better use of accuracy data in land change studies: estimating accuracy and area and quantifying uncertainty using stratified estimation. Remote Sensing of Environment, Vol. 129, pp. 122–131.

Olofsson, P., Foody, G. M., Herold, M., Stehman, S. V., Woodcock, C. E., and Wulder, M. A. 2014. Good practices for estimating area and assessing accuracy of land change. Remote Sensing of Environment, Vol. 148, pp. 42–57. doi: 10.1016/j.rse.2014.02.015.

Pflugmacher, D., Cohen, W. B., and Kennedy, R. E. 2012. Using Landsat-derived disturbance history (1972–2010) to predict current forest structure. Remote Sensing of Environment, Vol. 122, pp. 146–165.

R Development Core Team (2014). R: A language and environment for statistical computing, Vienna, Austria. Available at:. http://www.R-project.org/

Roy, D., et al., 2014. Landsat-8: Science and product vision for terrestrial global change research. Remote Sensing of Environment, 154-172.

Schmidt, G. L., Jenkerson, C. B., Masek, J., Vermote, E., & Gao, F. 2013. Landsat ecosystem disturbance adaptive processing system (LEDAPS) algorithm description. 17 (Retrieved from http://pubs.usgs.gov/of/2013/1057/).

Senf, C., Leitao, P. J., Pflugmacher, D., van der Linden, S., and Hostert, P. 2015. Mapping land cover in complex Mediterranean landscapes using Landsat: Improved classification accuracies from integrating multi-seasonal and synthetic imagery. Remote Sensing of Environment, Vol. 156. 527-536, DOI:10.1016/j.rse.2014.10.018.

Sexton, J. O. Urban, L. D., Donohue, M. J., Song, C. 2013. Long-term land cover dynamics by multi-temporal classification across the Landsat-5 record. Remote Sensing of Environment Vol. 128, pp. 246–258.

Tuner, D. P., Guzy, M., Lefsky, M. A., Ritts, W. D., Van Tuyl, S., & Law, B. E. 2004. Monitoring forest carbon sequestration with remote sensing and carbon cycle modeling. Environmental Management, Vol. 33, No. 4, pp. 457-466.

White, J.C., Wulder, M.A. 2013. The Landsat observation record of Canada: 1972–2012. Canadian Journal of Remote Sensing. Vol. 39, pp. 455–467.

White, J. C., Wulder, M. A., Hobart, G. W., Luther J. E., Hermosilla, T., Griffiths, P., Coops, N. C., Hall, R. J., Hostert P., Dyk, A. and Guindon L. 2014. Pixel-Based Image Compositing for Large Area Dense Time Series Applications and Science. Canadian Journal of Remote Sensing, Vol. 40, pp. 192–212.

Woodcock, C.E., Allen, R., Anderson, M., Belward, A., Bindschadler, R., Cohen, W., Gao, F., Goward, S.N., Helder, D., Helmer, E., Nemani, R., Oreopoulos, L., Schott, J., Thenkabail, P.S.,

Vermote, E.F., Vogelmann, J., Wulder, M.A., and Wynne, R. 2008. Free access to Landsat imagery. Science, Vol. 320, No. 5879 1011.

Wulder, M.A, W. Kurz, and M. Gillis, 2004. National level forest monitoring and modeling in Canada, Progress in Planning. Vol. 61, pp. 365-381.

Wulder, M.A., S. Franklin, J.C. White, J. Linke, and S. Magnussen. 2006. An accuracy assessment framework for large-area land cover classification products derived from medium resolution satellite data, International Journal of Remote Sensing, Vol. 27, pp. 663-683.

Wulder , M., A., and S. E. Franklin. 2007. Understanding Forest Dynamics: Remote Sensing and GIS Approaches. Taylor and Francis.

Wulder, M., and Nelson, T., 2003. EOSD land cover classification legend report. Version 2. Canadian Forest Service/TNT Geoservices, 83 pp. http://www.pfc.forestry.ca/eosd/cover/EOSD_legend_re-port-v2.pdf.

Wulder, M. A., White, J. C. Magnussen, S., and McDonald S. 2008. Validation of a large area land cover product using purpose-acquired airborne video. Remote Sensing of Environment, Vol. 106, pp. 480 – 491.

Wulder, M.A., J.C. White, and N.C. Coops. 2011. Fragmentation regimes of Canada's forests. The Canadian Geographer. Vol. 55, No. 3, pp. 288–300.

Wulder, M.A., Masek, J.G., Cohen, W.B., Loveland, T.R., Woodcock, C.E., 2012. Opening the archive: How free data has enabled the science and monitoring promise of Landsat. Remote Sensing of Environment, Vol. 122, pp. 2-10.

Yemshanov, D.; McKenney, D. W., and Pedlar, J. H. 2011. Mapping forest composition from the Canadian National Forest Inventory and land cover classification maps. Environmental Monitoring and Assessment, Vol. 184, pp. 4655-4669.

Zhu, Z., & Woodcock, C. E. 2012. Object-based cloud and cloud shadow detection in Landsat imagery. Remote Sensing of Environment, Vol. 118, pp.83–94. http://dx.doi.org/10.1016/j.rse.2011.10.028 .

Zhu, Z., and Woodcock, C. E. Continuous change detection and classification of land cover using all available Landsat data, 2014. Remote Sensing of Environment, Vol. 144, pp. 152–171.

Table 1. Variables derived from the BAP composites that were used as inputs for the land cover classification; the first layer is elevation from the DEM, followed by four Landsat spectral bands, two proxy composite vegetation indices, and 14 NBR based disturbance metrics derived from the Landsat time-series.

	Type	Variable	Description
Scenario 1: Single date inputs only	Topography	DEM	Digital Elevation Model
	Landsat spectral data	Red	Landsat Band 3
		NIR	Landsat Near Infrared (Band 4)
		SWIR	Landsat Shortwave Infrared (Band 5)
		SWIR	Landsat Shortwave Infrared (Band 7)
	Vegetation indices	NDVI	Normalized Difference Vegetation Index
		NBR	Normalized Burn Ratio
Scenario 2: Single date inputs plus trajectory-based change metrics	Time series (NBR-based) disturbance metrics	Trend type	Characterize the type of trends according to: Monotonic trends (no change or breakpoint), single breakpoint or disturbed.
		NBR RSME	Root square mean error of fitting the trend to the observed pixel-series values
		Trend magnitude	Difference between the 1st and the last value of the fitted trends
		Greatest disturbance year	The year for the greatest disturbances
		Greatest disturbance magnitude	NBR variation during the disturbance segment
		Greatest disturbance duration	Persistence of the disturbance event
		Pre-disturbance magnitude	Variation of the NBR from the initial date to the disturbance
		Post-disturbance magnitude	Variation of the NBR from the disturbance to end date
		Pre-disturbance duration	Duration of the pre disturbance
		Post-disturbance duration	Duration of the post disturbance
		Pre-disturbance monotonic trend duration	Continual trends before the disturbance segment
		Post-disturbance monotonic trend duration	Continual trends after the disturbance segment
		Pre-disturbance monotonic trend magnitude	
		Post-disturbance monotonic trend magnitude	

Table 2. Number of calibration and reverence pixels for different land-cover classes based on the EOSD LC 2000 land cover classification legend; samples were selected randomly and interpreted in the available colour-infrared aerial orthophotography acquired in 2007.

Class name	Class area (ha)	Calibration sample size	Reference sample size
Mixedwood	29919	138	59
Coniferous	21292	102	44
Herb	6424	40	17
Wetland treed	6220	39	17
Broadleaf	4778	33	14
Water	2671	24	10
Wetland	1008	17	7
Exposed land	296	14	6
Total		**406**	**174**

Table 3. Accuracy assessment of change detection identified by the trajectory analysis for years between 1990 and 2010 based on 200 sample pixels examined in the image data and available colour-infrared aerial orthophotography. Cell entries are expressed as the estimated area proportion of the cells of the error matrix.

		REFERENCE				
		Change	**No Change**	**Total**	**User's Accuracy**	**Commission Error**
PREDICTED	**Change**	0.093	0.013	0.105	88.00%	12.00%
	No change	0.063	0.832	0.895	93.00%	7.00%
	Total	0.155	0.845	1		
	Producer's Accuracy	59.71%	98.50%	**Overall Accuracy**		**92.47%**
	Omission error	40.29%	1.50%	**Margin of Error ±**		**3.66%**

Table 4. Error matrix of estimated area proportions for eight EOSD LC 2000 land cover classes using single date spectral variables and indices with 174 reference samples (interpreted in the available 1:20000 scale aerial orthophotographs). Cell entries are expressed as the estimated area proportion of the cells of the error matrix. Accuracy measures are presented with a 95% confidence interval.

		REFERENCE										
	Class name	**Mixedwood**	**Coniferous**	**Herb**	**Wetland Treed**	**Broadleaf**	**Water**	**Wetland**	**Exposed Land**	**Total**	**User's Accuracy (%)**	**Commission Error (%)**
PREDICTED	**Mixedwood**	0.285	0.025	0.031	0.031	0.019	0	0	0.006	0.397	71.88%	28.13%
	Coniferous	0.042	0.278	0	0	0	0	0	0	0.320	86.96%	13.04%
	Herb	0.018	0	0.072	0	0	0	0	0	0.090	80.00%	20.00%
	Wetland Treed	0.018	0	0	0.050	0	0	0.005	0	0.073	68.75%	31.25%
	Broadleaf	0.005	0	0	0	0.050	0	0	0	0.055	90.91%	9.09%
	Water	0	0	0	0	0	0.039	0	0	0.039	100.00%	0.00%
	Wetland	0	0	0	0.002	0	0	0.014	0	0.016	85.71%	14.29%
	Exposed Land	0	0	0.004	0	0.001	0	0	0.005	0.009	50.00%	50.00%
	Total	0.368	0.303	0.107	0.083	0.070	0.039	0.018	0.011	1		
	Producer's accuracy (%)	77.43%	91.83%	67.55%	60.08%	71.97%	100.00%	75.05%	43.27%	**Overall accuracy**		**79.38%**
	Omission error (%)	22.57%	8.17%	32.45%	39.92%	28.03%	0.00%	24.95%	56.73%	**Margin of Error ±**		**6.01%**

Table 5. Error matrix of estimated area proportions for eight EOSD LC 2000 land cover classes using combination of single date spectral variables and time series disturbance metrics with 174 reference samples (interpreted in the available 1:20000 scale aerial orthophotographs). Cell entries are expressed as the estimated area proportion of the cells of the error matrix.

		REFERENCE										
	Class name	**Mixedwood**	**Coniferous**	**Herb**	**Wetland Treed**	**Broadleaf**	**Water**	**Wetland**	**Exposed Land**	**Total**	**User's Accuracy (%)**	**Commission Error (%)**
PREDICTED	**Mixedwood**	0.336	0.020	0.013	0.020	0.007	0	0	0	0.397	84.75%	15.25%
	Coniferous	0.027	0.274	0.020	0	0	0	0	0	0.320	85.42%	14.58%
	Herb	0.014	0	0.077	0	0	0	0	0	0.090	84.62%	15.38%
	Wetland Treed	0.009	0	0	0.059	0	0	0.005	0	0.073	81.25%	18.75%
	Broadleaf	0.004	0	0	0	0.051	0	0	0	0.055	92.86%	7.14%
	Water	0	0	0	0	0	0.039	0	0	0.039	100.00%	0.00%
	Wetland	0	0	0	0.002	0	0	0.014	0	0.016	85.71%	14.29%
	Exposed Land	0	0	0.001	0	0	0	0	0.008	0.009	85.71%	14.29%
	Total	0.390	0.294	0.111	0.082	0.058	0.039	0.018	0.008	1		
	Producer's accuracy (%)	86.24%	93.13%	68.74%	72.50%	88.40%	100.00%	75.05%	100.00%	**Overall accuracy**		**85.77%**
	Omission error (%)	13.76%	6.87%	31.26%	27.50%	11.60%	0.00%	24.95%	0.00%	**Margin of error ±**		**5.19%**

Table 6. Illogical class transitions used in the transition-rule filter. Acceptable class transition in the center year between the start and end year class is indicated with "✓", while Illogical transitions are indicated with "×".

		Middle (second) year							
	Class	Mixedwood	Coniferous	Herb	Wetland Treed	Broadleaf	Water	Wetland	Exposed Land
Start (first) and end (third) year	Mixedwood	✓	×	✓	×	×	×	×	×
	Coniferous	×	✓	×	×	×	×	×	×
	Herb	✓	×	✓	×	×	×	×	✓
	Wetland Treed	×	×	×	✓	×	×	×	×
	Broadleaf	×	×	×	×	✓	×	×	×
	Water	×	×	✓	×	×	✓	✓	✓
	Wetland	×	×	✓	×	×	✓	✓	✓
	Exposed Land	×	×	✓	×	×	✓	✓	✓

Table 7. Error matrix of estimated area proportions for the transition-rule filtered land cover map for the reference year 2007. The classification for this map was performed using a combination of single date spectral variables and time series disturbance metrics (Table 1). Cell entries are expressed as the estimated proportion of area.

		REFERENCE										
	Class name	**Mixedwood**	**Coniferous**	**Herb**	**Wetland Treed**	**Broadleaf**	**Water**	**Wetland**	**Exposed Land**	**Total**	**User's Accuracy (%)**	**Commission Error (%)**
PREDICTED	**Mixedwood**	0.343	0.013	0.013	0.020	0.007	0	0	0	0.397	86.44%	13.56%
	Coniferous	0.020	0.294	0.007	0	0	0	0	0	0.320	91.67%	8.33%
	Herb	0.014	0	0.077	0	0	0	0	0	0.090	84.62%	15.38%
	Wetland Treed	0.018	0	0	0.055	0	0	0	0	0.073	75.00%	25.00%
	Broadleaf	0.004	0	0	0	0.051	0	0	0	0.055	92.86%	7.14%
	Water	0	0	0	0	0	0.039	0	0	0.039	100.00%	0.00%
	Wetland	0	0	0	0.002	0	0	0.014	0	0.016	85.71%	14.29%
	Exposed Land	0	0	0.001	0	0	0	0	0.008	0.009	85.71%	14.29%
	Total	0.399	0.307	0.098	0.077	0.058	0.039	0.014	0.008	1		
	Producer's accuracy (%)	85.94%	95.62%	78.10%	70.87%	88.40%	100.00%	100.00%	100.00%	**Overall accuracy**		**87.98%**
	Omission error (%)	14.06%	4.38%	21.90%	29.13%	11.60%	0.00%	0.00%	0.00%	**Margin of error ±**		**4.83%**

Table 8. Land cover class transitions (%) by 5-year epochs in the Hearst Forest.

	Epoch 1 (1990-1995), Epoch 2 (1995-2000), Epoch 3 (2000-2005), Epoch 4 (2005-2010)						
	To						
From	Mixedwood	Coniferous	Herb	Wetland Treed	Broadleaf	Wetland	Exposed Land
Mixedwood							
Epoch 1	28.61	0.66	51.56	3.91	5.68	4.49	5.10
2	8.65	0.47	71.30	1.69	0.42	2.21	15.26
3	10.19	1.17	56.74	2.13	0.38	9.12	20.26
4	21.53	4.05	38.55	11.45	1.90	9.25	13.28
Coniferous							
Epoch 1	10.19	23.90	56.53	2.36	0.26	4.13	2.63
2	1.90	10.58	70.40	1.61	0.02	4.65	10.83
3	4.28	4.52	56.94	2.31	0.07	13.65	18.23
4	7.76	8.33	34.62	10.67	0.75	16.48	21.40
Herb							
Epoch 1	16.59	0.42	80.04	0.92	0.53	0.47	1.03
2	3.19	1.32	88.04	1.16	0.61	1.53	4.16
3	3.44	0.50	80.46	0.95	0.08	2.87	11.70
4	13.50	3.78	65.59	4.85	0.72	5.84	5.72
Wetland Treed							
Epoch 1	24.50	0.43	60.28	3.21	1.48	5.77	4.32
2	6.31	1.17	71.81	3.11	0.10	4.52	12.97
3	5.57	1.86	63.83	4.95	0.09	10.99	12.71
4	9.49	4.02	32.92	23.36	1.74	18.72	9.74
Broadleaf							
Epoch 1	28.16	0.17	49.55	0.73	6.16	5.94	9.29
2	5.33	0.18	73.62	0.24	3.46	2.39	14.77
3	7.52	0.26	51.47	1.38	32.54	1.89	4.92
4	10.62	6.06	56.31	3.44	4.67	6.08	12.81
Wetland							
Epoch 1	31.70	0.64	29.90	1.85	4.61	26.33	4.97
2	7.80	6.84	43.33	5.48	0.41	20.88	15.28
3	7.20	2.93	39.20	4.20	0.70	30.08	15.70
4	12.81	8.85	16.32	16.29	1.94	33.11	10.69
Exposed Land							
Epoch 1	16.20	0.27	35.99	1.09	3.21	9.01	34.23
2	2.21	1.38	19.75	0.71	3.59	1.12	71.24
3	2.20	0.37	29.45	0.89	0.21	2.13	64.76
4	6.88	1.12	46.89	4.57	0.87	4.31	35.36

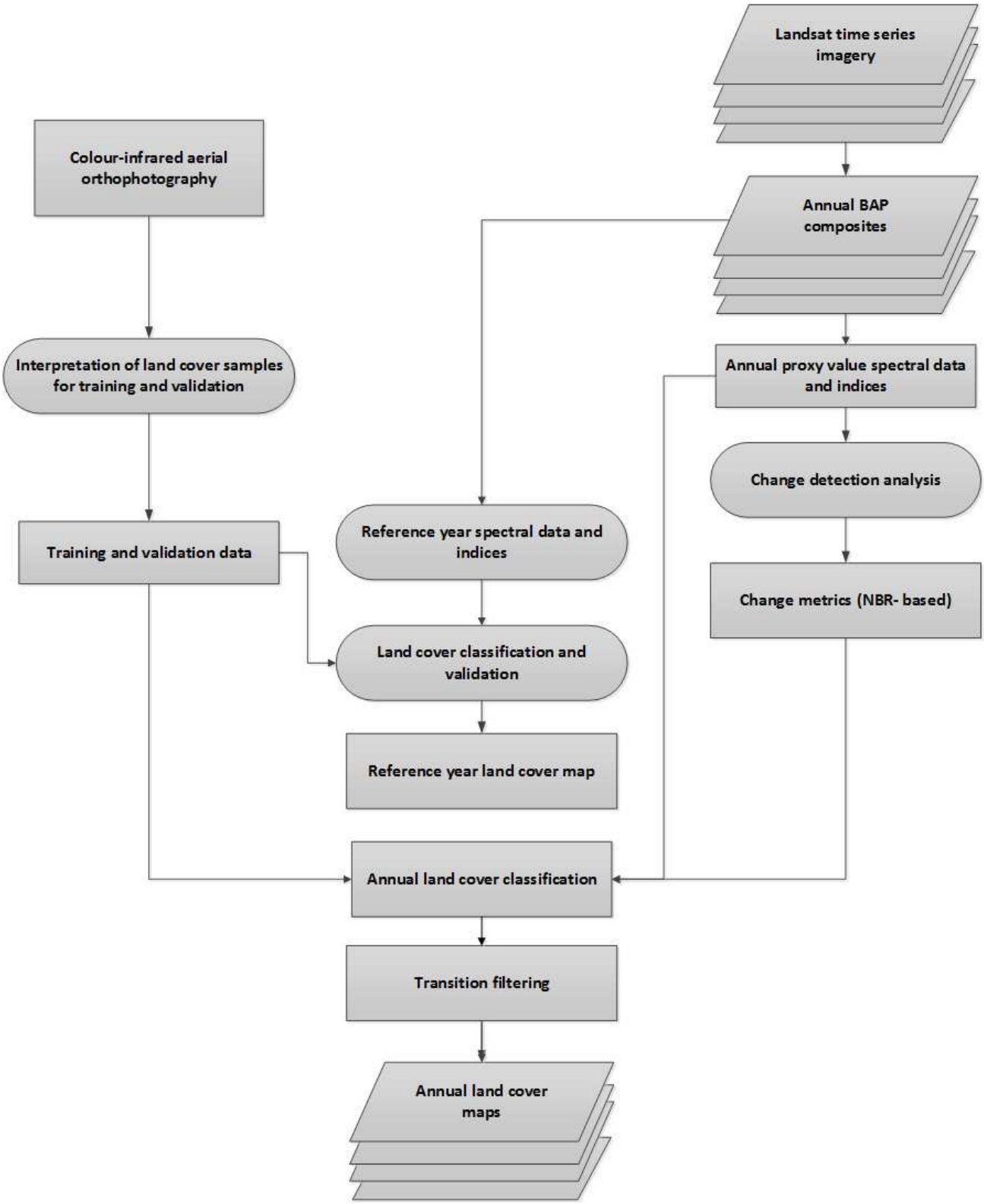

Figure 1. A flowchart of the overall approach for the annual land cover classification.

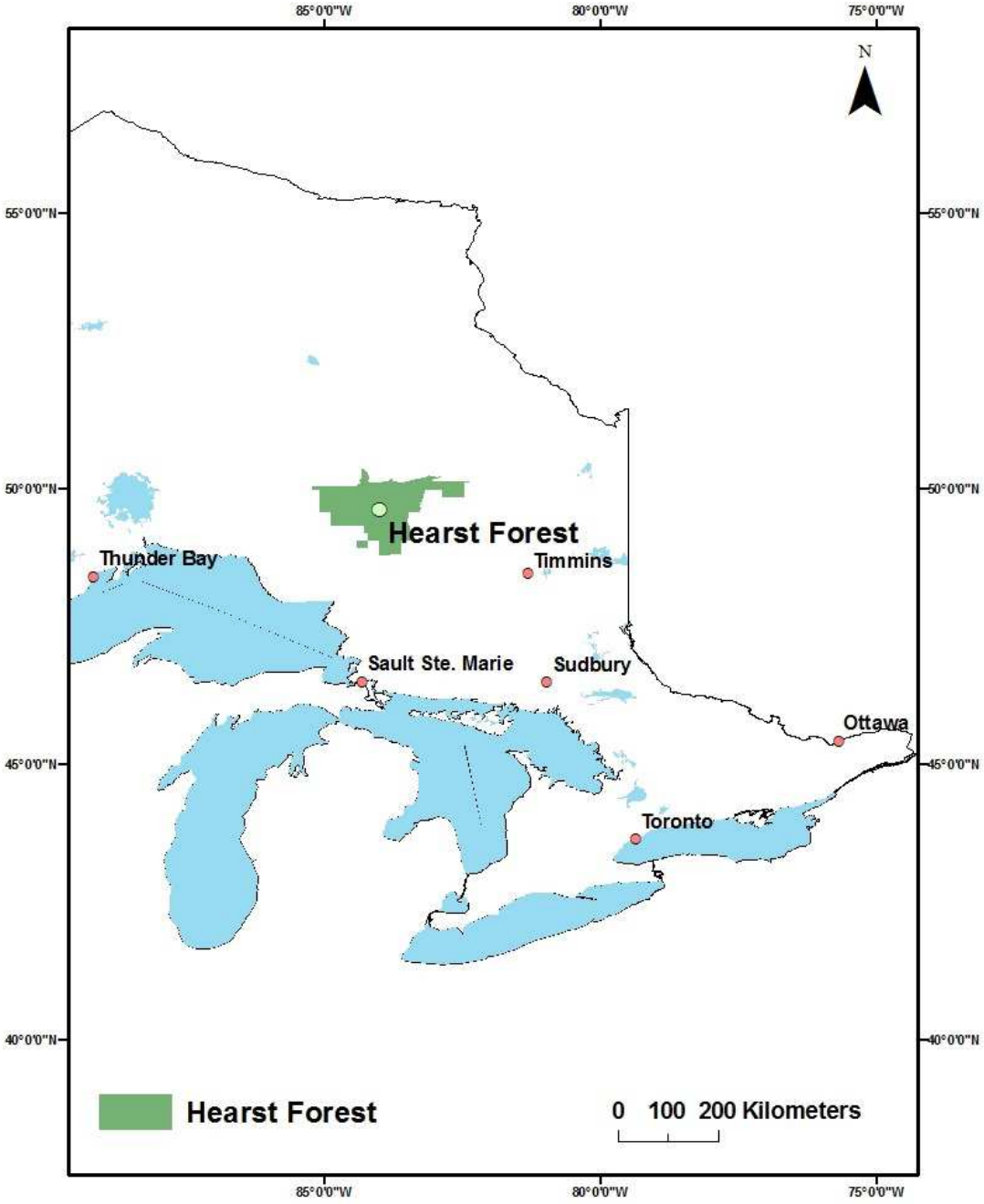

Figure 2. The location of the study area within the Hearst Forest Management Area in northern Ontario.

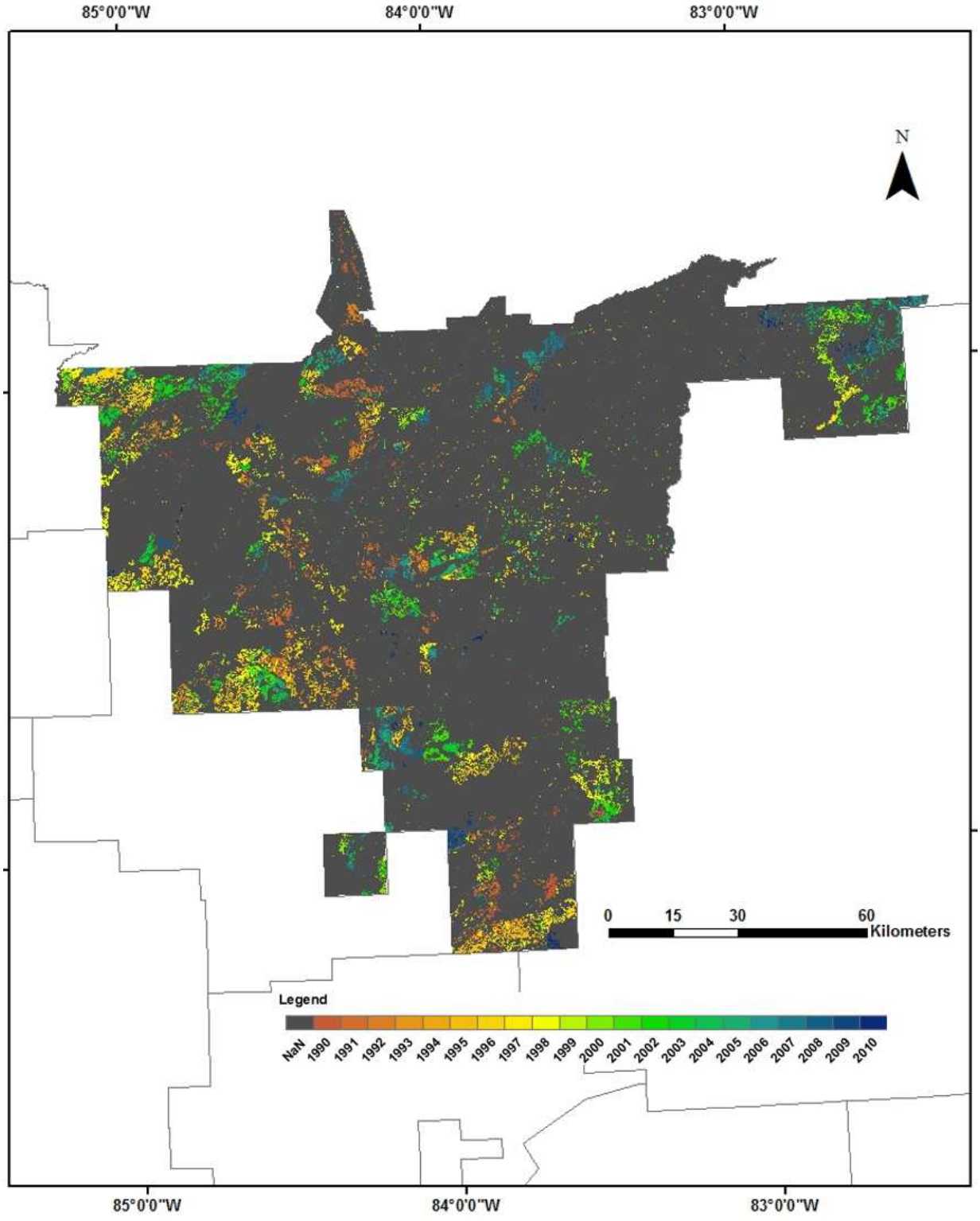

Figure 3. Hearst Forest land cover change map showing land cover changes detected through greatest change metric during the time period 1990-2010.

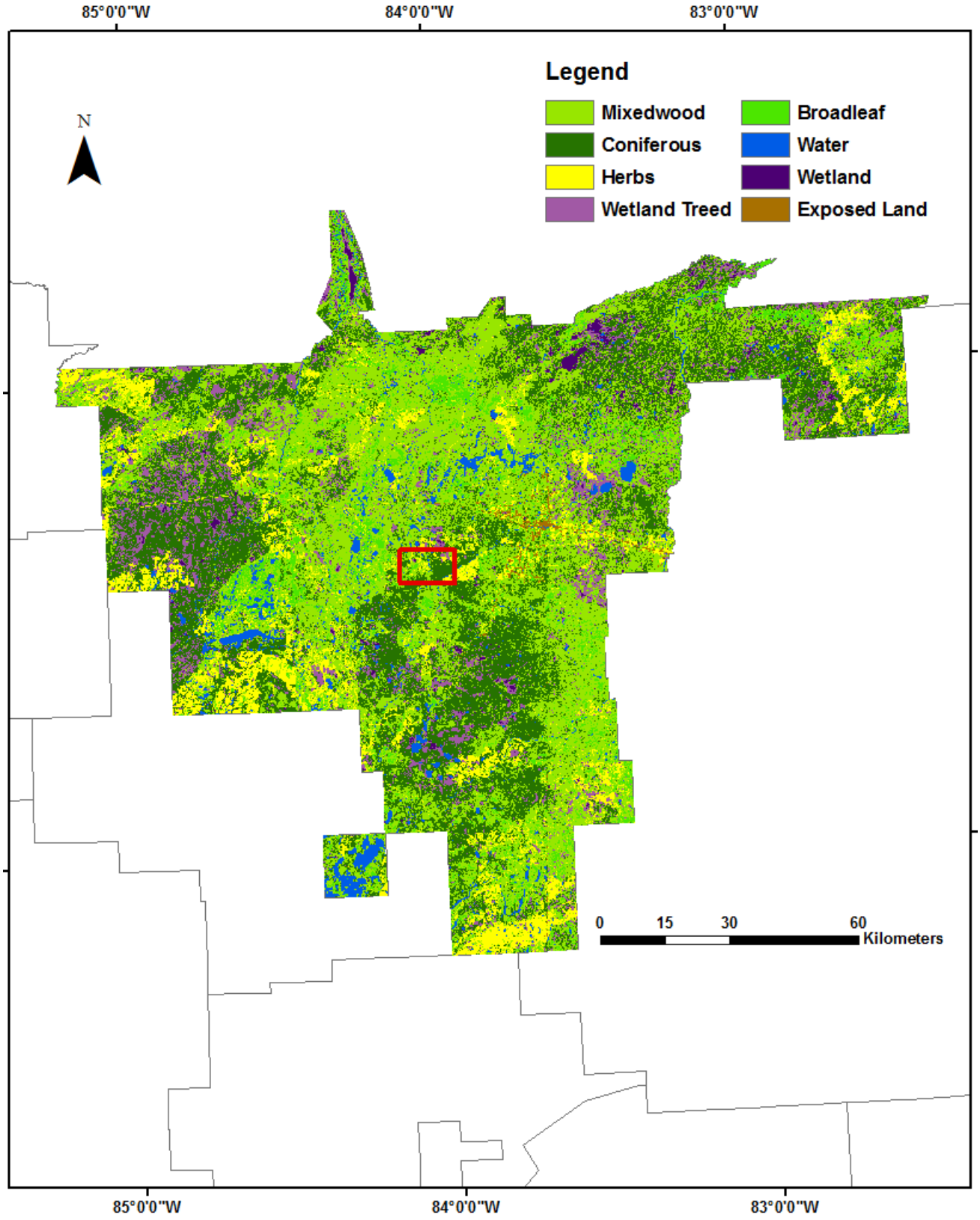

Figure 4. Eight-class land cover classification in 2007 of the Hearst Forest study area in northern Ontario based on Landsat spectral data and time series disturbance metrics. Overall land cover classification accuracy was approximately 86% based on 174 reference sites. The small window outlined at the center of the map is the area shown in more detail in Figures 6, 7 and 8.

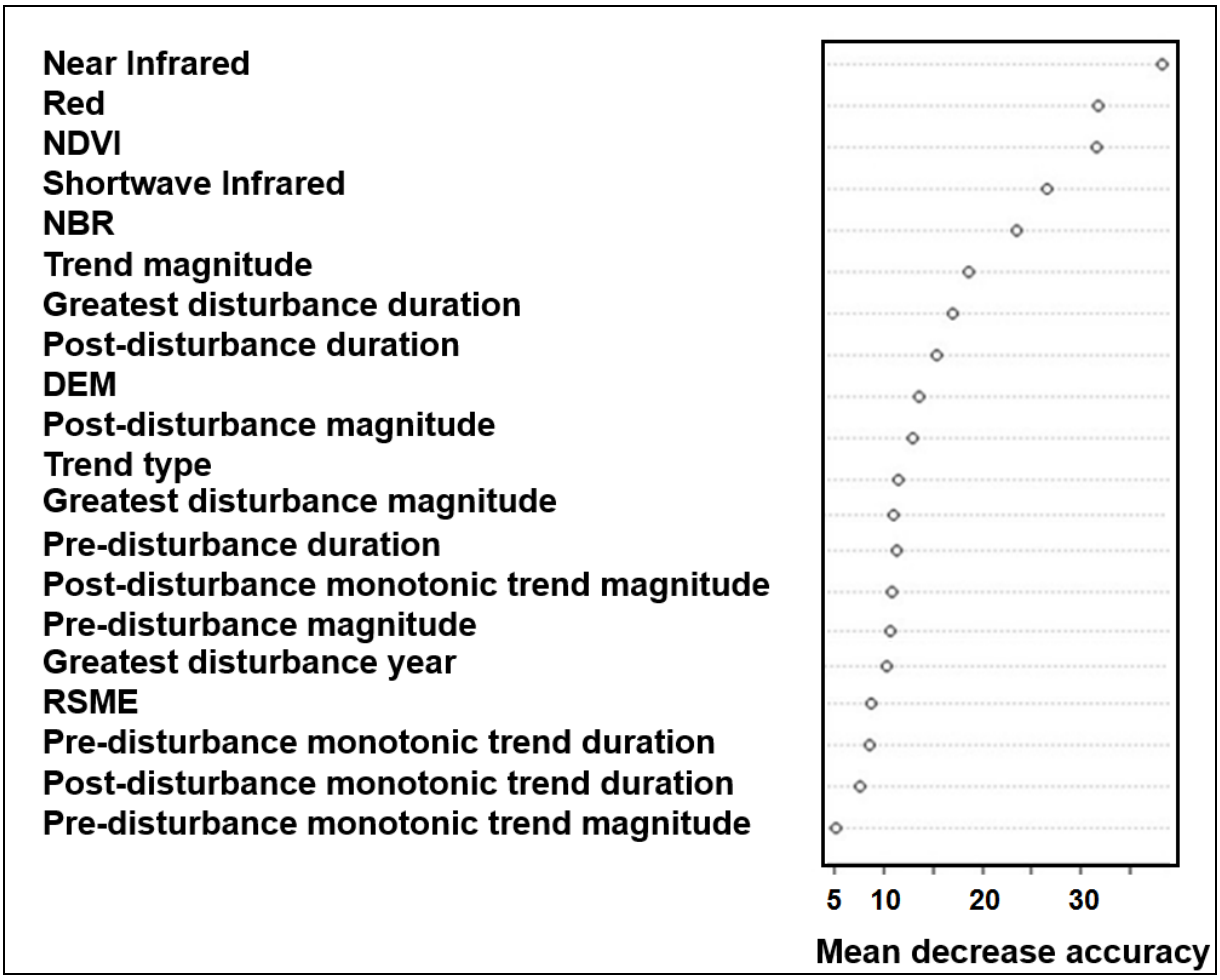

Figure 5. Training data variable importance (VI) as estimated in the RF classifier; VI is the average of the squared classification error when the variable in the classification is replaced (permuted) with a random one, and is an indication of the variables' contribution to the classification accuracy.

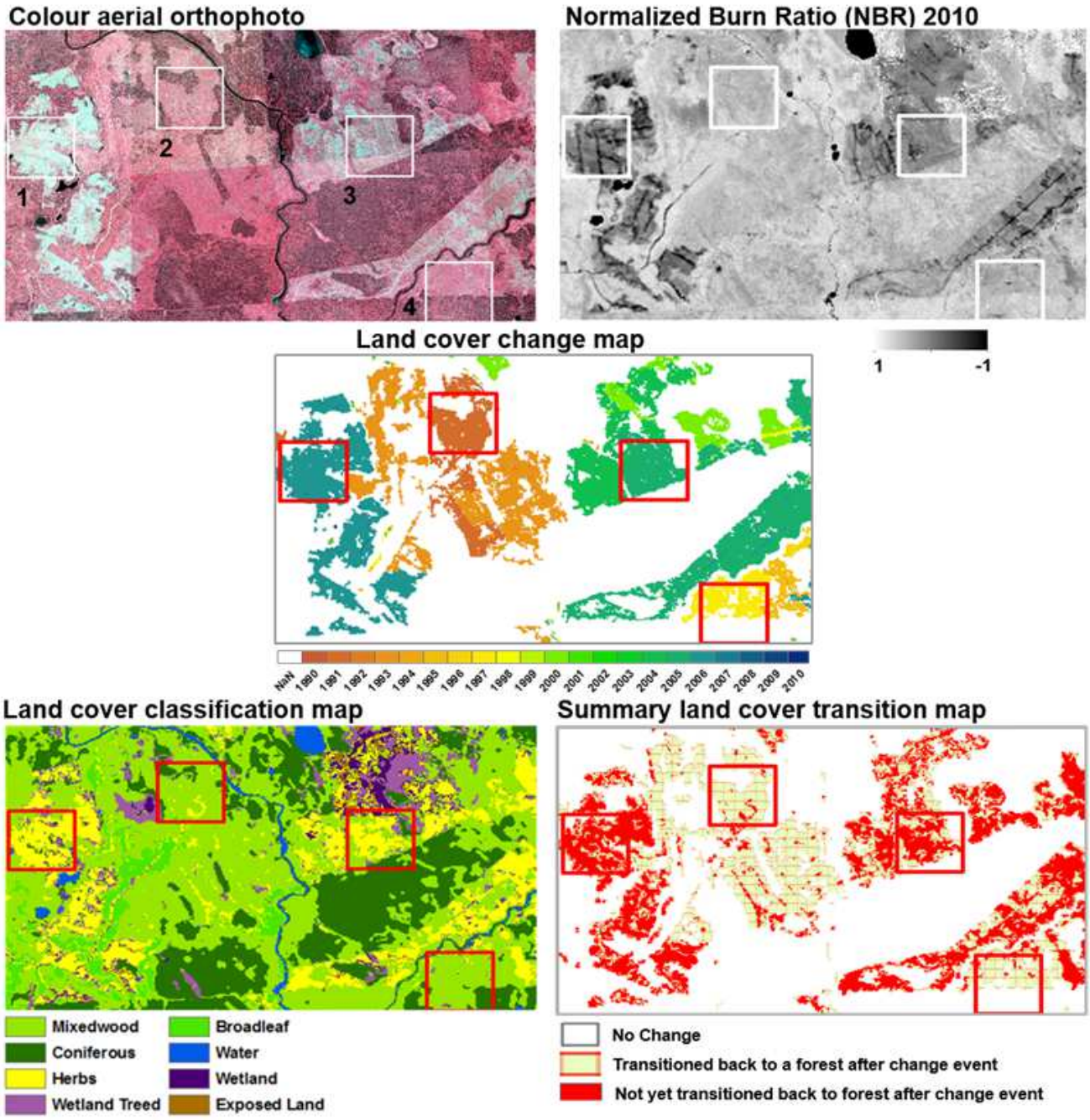

Figure 6. A sub-area of the Hearst Forest dataset showing exemplars of the various land cover transitions in the study area. Shown are the colour-infrared aerial photography, normalized burn ratio (NBR), land cover changes over the 1990-2010 time period, eight-class land cover classification for 2010, and a binary recovery no-recovery mask. Sites 2 and 4 were disturbed early in the time series 1991 and 1997, respectively; sites 1 and 3 are more recent disturbances (2006 and 2005, respectively). Sites 2 and 3 are shown in greater detail in Figures 7 and 8 respectively.

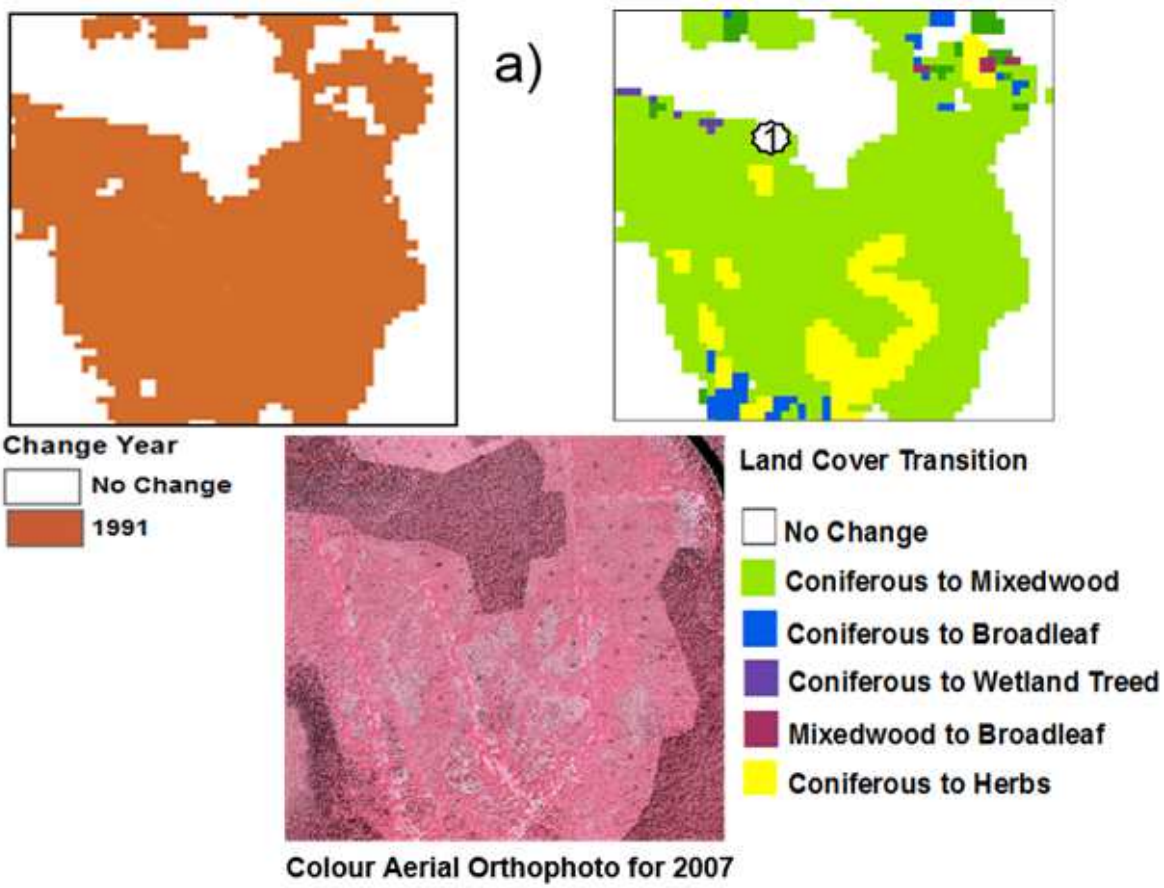

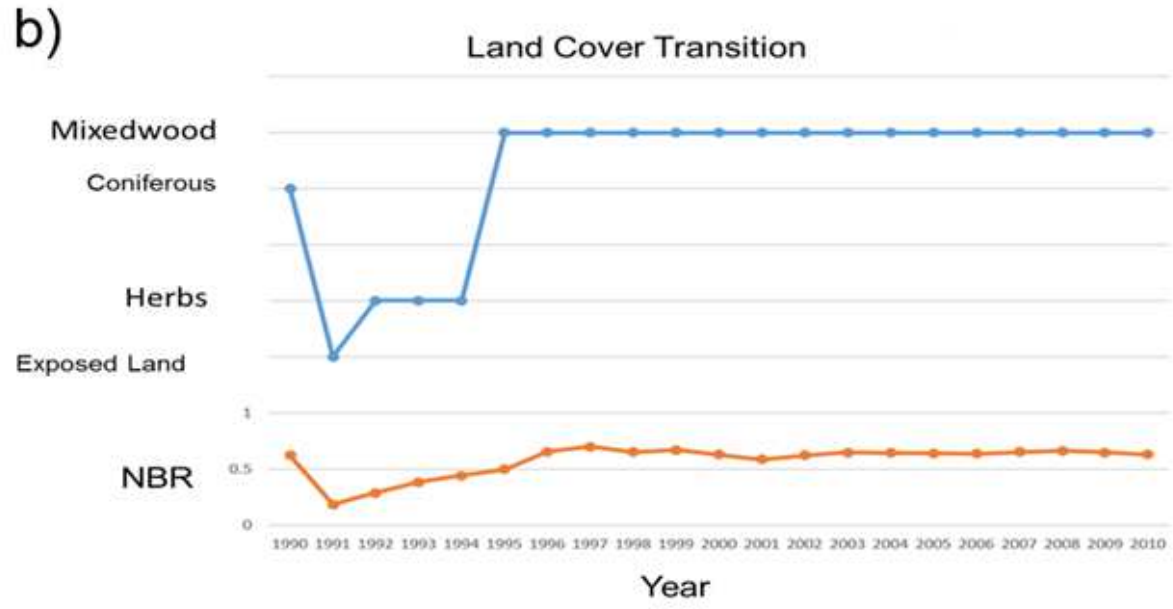

Figure 7. Examples of land cover transitions in areas shown in Figure 6: a) and b) show site 2, this site contains an area that was clearcut at the beginning of the available time series; at that time, the dominant land cover class was coniferous, and the majority of the area was converted to mixedwood at the end of the time period. The graph in 7b) shows the land cover transitions for a pixel located near the edge of this cutover in site 2 where the land cover has transitioned from coniferous to exposed land and then to herb and finally to mixedwood.

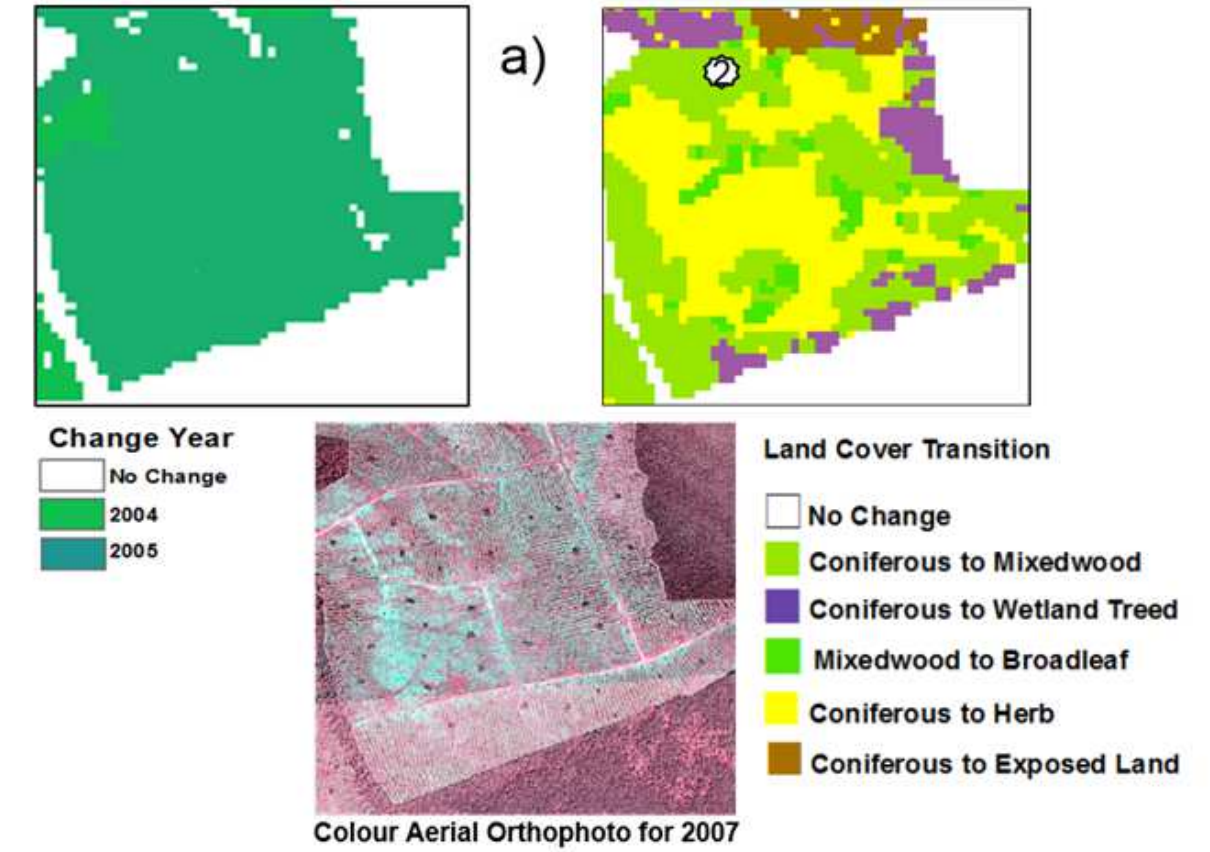

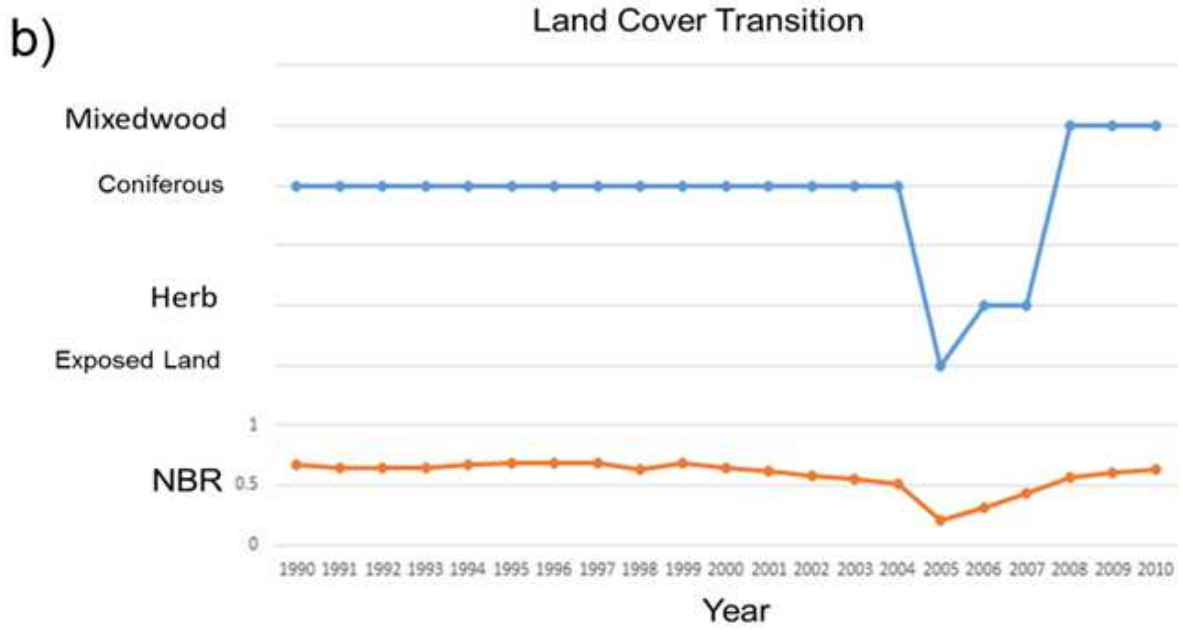

Figure 8. Site 3 in Figure 6. Site 3 has experienced land cover change in 2004 and 2005, and many of these cutover pixels transitioned to different land cover classes by the end of the time series. The graph in 8b) shows a pixel that began as conifer, transitioned to exposed land following harvesting, and subsequently transitioned from herb to mixedwood.

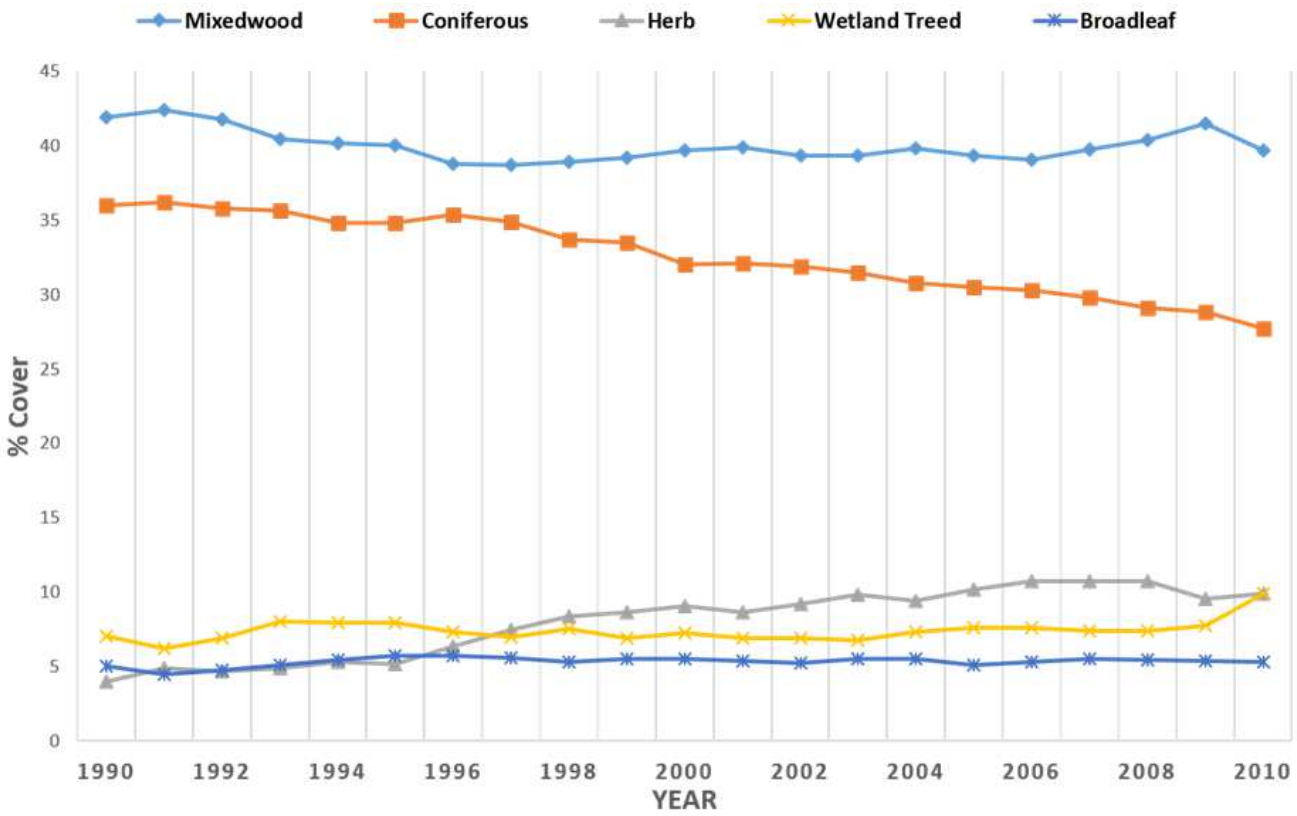

Figure 9. Areal percentage of the five major land-cover classes mixedwood, coniferous, herb, wetland treed, and broadleaf for years 1990 to 2010.